5-12-2022

Amplitude-modulated cVEMP (AMcVEMPs) versus transient cVEMP response properties: Possible implications

Andrew Thorne
James Madison University

Amplitude-Modulated cVEMP (AMcVEMPs) Versus Transient cVEMP Response Properties: Possible Implications

by Andrew Thorne

A dissertation submitted to the Graduate Faculty of

JAMES MADISON UNIVERSITY

In

Partial Fulfillment of the Requirements

for the degree of

Doctor of Audiology

Department of Communication Sciences and Disorders

May 2022

FACULTY COMMITTEE:

Committee Chair:
Christopher Clinard, PhD

Committee Members/ Readers:

Christopher Clinard, PhD

Erin Piker, PhD

Lincoln Gray, PhD

Table of Contents

Abstract iv
Introduction 1
Methods 4
Participants 4
Stimuli 5
Procedure 6
AMcVEMP Analysis 7
Transient cVEMP Analysis 9
Statistical Approach 10
Results 10
EMG Activation 10
Amplitude 11
Raw Amplitude 11
Corrected amplitudes 12
Signal to Noise Ratio 15
Relationship Between Amplitude and Noise 15
Phase Coherence 17
Interaural Asymmetry Ratios 18
AMcVEMP Amplitude vs. Transient Amplitude 20
Discussion 20
Amplitude 20
Transient cVEMP and AMcVEMP Comparisons 20
SNR and Phase Coherence 21
SNR Plateaus 21
Phase Coherence 22
Clinical Implications 22
Advantages of Bone Conduction 22
Maximum SNR and PC Reached With Low EMG 23
Interaural Asymmetry Ratios are Lower for AMcVEMPs 23
Nonlinear Behavior of AMcVEMPs 24

Conclusion 25
References 26

List of Figures

Figure 1: Example stimuli for both transient and AMcVEMPs 6
Figure 2*:* Individual transient and AMcVEMP data 9
Figure 3*:* Scatterplots of EMG target and EMG activation. 11
Figure 4*:* AMcVEMP amplitude across EMG targets 13
Figure 5: Transient cVEMP amplitude across EMG targets 14
Figure 6*:* Scatterplots of AMcVEMP and transient cVEMP amplitude…… 14
Figure 7: AMcVEMP SNR across EMG targets.. 16
Figure 8: Log-scale of amplitude and noise increase over EMG targets 17
Figure 9*:* Phase coherence across EMG target 18
Figure 10: Boxplots of Asymmetry Ratios from each EMG target 19

Abstract

Cervical vestibular evoked myogenic potentials (cVEMPs) elicited by steady-state amplitude-modulated (AM) tones yield different information than conventional cVEMPs elicited by transient tonebursts, such as signal-to-noise ratio (SNR) and phase coherence (PC). This study systematically examined the effects of tonic EMG activation on AMcVEMP response properties versus conventional transient cVEMPs. Thirty five young, healthy adults (ages 19–23) with normal audiograms and no known vestibular lesions participated in this study. AMcVEMPs were elicited with bone-conducted tones with a carrier frequency of 500 Hz and an amplitude modulation frequency of 37 Hz, and transient cVEMPs were elicited by 4-0-4 Blackman-gated 500 Hz tonebursts with 8 ms duration. Both cVEMP types were recorded for five different EMG target levels ranging from 10 to 90 μV. For both cVEMP types, amplitude increased linearly with increased tonic EMG activation. Corrected amplitude, SNR, and PC values were minimal at 10 μV, but were robust and virtually plateaued in value from 30 to 90 μV. Interaural asymmetry ratios (IARs) for SNR and phase coherence were substantially lower than either raw or corrected amplitude measures. SNR, PC, and EMG-corrected amplitudes reached essentially maximum values at relatively low levels of EMG activation and did not require higher levels of EMG activation to be adequately elicited. Lower IARs for SNR and PC could have clinical implications about their ability to detect unilateral saccular and/or inferior vestibular nerve lesions versus conventionally used

amplitude measures. Findings of this study largely replicated those of Clinard et al (2020).

Introduction

Otolith end organs, the saccule and utricle, respond to linear acceleration and gravity. However, acoustic and vibratory stimulation can also excite the otoliths and generate neuromuscular responses from various muscles throughout the body; when these responses are recorded from the sternocleidomastoid muscle (SCM) on the neck, they are called cervical vestibular evoked myogenic potentials (cVEMPs). Cervical VEMPs are inhibitory and represent the functioning of the saccule and the vestibulocollic reflex pathway (VCR) (Colebatch & Halmagyi, 1992) and they are typically elicited by transient click or toneburst stimuli. These responses are inhibitory in nature, and therefore require a certain amount of tonic electromyographic activation of the SCM to be measurable. Moreover, higher EMG levels correspond to higher cVEMP amplitudes (Akin et al., 2004; Lim et al., 1995). The response waveforms for cVEMPs are traditionally analyzed by examining their positive and negative peaks occurring at approximately 13 and 23 ms, respectively. This response waveform is commonly referred to as p13-n23 (Colebatch et al., 1994)

In clinical settings, cVEMP peak-to-peak amplitudes and peak latencies are often compared between left and right ears in order to determine the presence of unilateral weaknesses and lesions (Li et al., 2015; McCaslin et al., 2014). To minimize the false diagnosis of asymmetries between sides, it is

important to correct the raw cVEMP amplitude for the amount of EMG activity; commonly, this is done by dividing the p13-n23 amplitude for each individual sweep by the rectified mean of the patient's EMG at a pre-stimulus baseline (Bogle et al., 2013; McCaslin et al., 2014; S M Rosengren et al., 2010). Biofeedback methods can also be used to keep the patient's EMG activity within a certain range (Papathanasiou et al., 2014), such as the patient viewing a live bar graph of the EMG activity while the stimulus is being presented (Clinard et al., 2020), but this is not always performed clinically.

Transient cVEMPs elicited by brief tonebursts remain widely used as a clinical diagnostic test of saccular and VCR pathway function (Papathanasiou et al., 2014). More recently, it has been found that cVEMPs can also be elicited by long-duration, amplitude-modulated tones (Bell et al., 2010; Clinard et al., 2020; Oliveira et al., 2014). Contrary to conventional cVEMPs, amplitude-modulated cVEMPs (AMcVEMPs) utilize steady-state stimuli, which allows for the examination of cVEMP response properties beyond amplitude and latency. These include the signal-to-noise ratio (SNR) and phase-coherence (PC) of the response, which are analyzed via objective detection algorithms in a similar manner to ASSRs (Picton et al., 2003, Ross 2013).

Using this steady-state strategy, it is also possible to view the harmonics of the modulation frequency on the FFT of the AMcVEMP response. Previous animal studies have found the presence of various distortion products in the saccules of bullfrogs (Jaramillo et al., 1993; Kozlov et al., 2011, 2012) and in mammals such as guinea pigs (Pastras et al., 2017) and rats (Songer & Eatock,

2013). These harmonics were shown to be a result of the gating compliance of saccular hair cells (Jaramillo et al., 1993; Kozlov et al., 2011). In humans, viewing the FFT of the AMcVEMP response could possibly allow the examiner to assess the presence of harmonic distortion products in the saccule, and therefore, the functioning of the saccular hair cells themselves.

In a recent study (Clinard et al., 2020) we reported response properties of the bone-conducted AMcVEMP evaluated in 14 young, female participants. Data showed that raw AMcVEMP amplitude scaled linearly with EMG activation similar to transient cVEMPs (Akin et al., 2004; Colebatch & Halmagyi, 1992; Noij et al., 2017). In contrast, AMcVEMP signal-to-noise ratio and phase coherence were robust at lower EMG levels (i.e., 30 µV) and remained constant through higher EMG levels (i.e, 90 µV); these findings indicate that larger levels of muscle activation do not benefit the SNR of the response, and that relatively low levels of muscle activation are adequate to detect robust AMcVEMPs. In addition, interaural asymmetry ratios (IARs) for SNR and PC were substantially lower than for amplitude analyses (Clinard et al., 2020). IARs for both corrected and uncorrected AMcVEMP amplitudes were consistent with common clinical cutoff criterion of approximately 45% (Li et al., 2015; McCaslin et al., 2014; Tilburg et al., 2014); however, IARs for SNR and PC had an upper limit of normal of approximately 15%. Because IARs are commonly used for the clinical evaluation of unilateral vestibular pathologies, this finding could potentially have important clinical implications regarding the sensitivity and specificity of the AMcVEMP as a diagnostic test of saccular and VCR pathway function. However, it is currently

unknown how the IARs for transient cVEMPs compare to the IARs of AMcVEMPs within the same participants and if smaller IARs for SNR and PC would be observed in a larger sample of young adults.

Sensory hair cells in the otolith organs of animals are known to have nonlinear processing, such as rectification (Holt & Eatock, 1995; Sugihara & Furukawa, 1989). Our recent work described the presence of harmonic distortion products from the stimulus modulation frequency, consistent with rectification at the level of the sensory hair cell (Clinard et al., 2020). Lastly, AMcVEMP responses at the harmonics of the modulation frequency (37 Hz, F0) were found with regularity, particularly at the second harmonic (H2).

The current study presents further findings on the effects of tonic EMG activation on basic characteristics of AMcVEMPs, in a larger sample of young healthy participants of both sexes. The purposes of this experiment included examining the effect of tonic EMG activation on: 1) AMcVEMP response characteristics of amplitude, SNR, and PC, 2) IARs of transient and amplitude-modulated cVEMPs within the same participants.

Methods

Participants

Thirty five young adults participated in this experiment (28 female, 7 male). The average participant age was 21.6 (std. err = 0.27, range 19-23). All participants had Type A tympanograms and audiometric thresholds within normal limits at octave frequencies from 250 to 8000 Hz. Detailed case histories were obtained to rule out participants self-reporting any history of neurological and/or

balance disorders. The initial ear of testing, left or right, was alternated for each participant. All methods and procedures used in this study were approved and in accordance with the Institutional Review Board at James Madison University.

Stimuli

AMcVEMPs were elicited by sinusoidally amplitude-modulated tones with a carrier frequency of 500 Hz and an amplitude-modulation frequency of 37.10938 Hz, which has been shown to elicit robust AMcVEMPs (Bell et al., 2010; Clinard et al., 2020) and minimizes overlap between response energy and 60 Hz harmonics. Coherent sampling was used to specify stimulus frequencies and limit the response to one FFT bin. Tone duration was 1024 ms. Stimuli were delivered at 65 dB HL (123 dB force level re: 1 μN) via a B81 bone vibrator (RadioEar) with its standard metal headband (ANSI, 2004). A Larson Davis AMC493B artificial mastoid with a Larson Davis 824 sound level meter, a 6-cc coupler (AEC 100), and a 4–5-N weight were used for calibration. Transient cVEMPs were elicited by a Blackman-gated 500 Hz toneburst with 8 ms duration (4-0-4 ms rise, plateau, fall), which has been shown to elicit robust cVEMPs (Romero et al., 2021). Tonebursts for transient cVEMPs were presented at 125 dB pFL, which was the pFL value for the AM tones; both stimuli were presented with equal dB pFL levels. Sampling rate for all stimuli was 44.1 kHz. Figure 1 illustrates both stimuli. All stimuli were presented in alternating polarity.

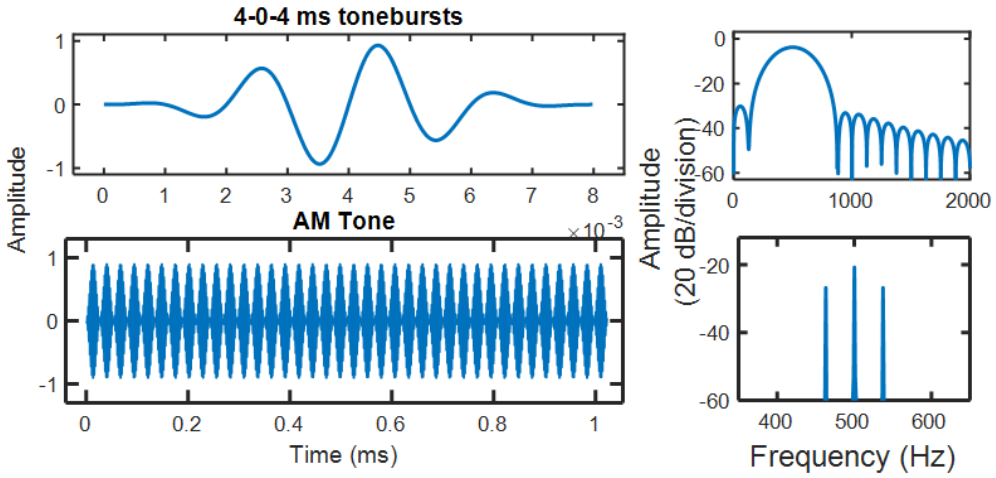

Figure 1: Example stimuli for both transient and AMcVEMPs. ***Top Left*****,** Time-based waveform of 4-0-4 Blackman-gated 500 Hz toneburst stimulus used to elicit transient cVEMPs. ***Top Right*****,** Frequency spectrum of 4-0-4 Blackman-gated 500 Hz toneburst stimulus used to elicit transient cVEMPs. ***Bottom Left*****,** Time-based waveform of steady-state tone with a carrier frequency of 500 Hz and an amplitude-modulation frequency of 37 Hz used to elicit AMcVEMPs. ***Bottom Right*****,** Frequency spectrum of amplitude-modulated tone used to elicit AMcVEMPs.

Procedure

Stimuli were delivered using a Neuroscan Stim2 system and recordings were obtained using a Neuroscan RT system with Curry 8 acquisition software (Compumedics). Disposable snap electrodes were used for one-channel recordings (Ambu Neuroline 720). Electrode positions were at the midpoint of the sternocleidomastoid muscle (noninverting) and the sternoclavicular junction, with the ground electrode at Fpz. Bandpass filters were 5–5000 Hz. Sampling rate was 20 kHz. Artifact rejection was not used.

Five EMG target levels of 10, 30, 50, 70, and 90 μV were assessed. Participants monitored their live, full-wave rectified EMG of their

sternocleidomastoid muscle (S M Rosengren et al., 2010) by viewing a live, real-time bar graph of their EMG throughout the recording (Akin et al., 2004). This monitoring was achieved by passing EMG data from Curry acquisition software to Matlab. Participants remained in a seated position while turning their heads until the rectified EMG from their sternocleidomastoid muscles reached the target line of activation. Participants had the opportunity to practice sufficiently reaching and maintaining the EMG target prior to the first recording. Participants were also coached as necessary on maintaining EMG throughout the recording process.

Each ear was tested separately. The order of ear testing and EMG target level were randomized. The B81 bone vibrator was placed 3 cm posterior and 2 cm superior to the external auditory meatus to obtain maximum cVEMP amplitudes (Welgampola et al., 2003). A spring scale (Ohaus 8003-PN) was used for each participant to verify that the headband applied 5.4 (+ 0.5) N of force (ANSI 2004). Breaks were provided for every participant to prevent fatigue. Data collection was performed in one 2 hour session. For AMcVEMPs, interstimulus interval was 109 ms, corresponding to a rate of 0.937/s. Each recording consisted of 128 sweeps and lasted approximately 2.3 min. For transient cVEMPs, stimulus rate for transient cVEMPs was 4.8 tonebursts/sec, and each recording lasted approximately 25 seconds.

AMcVEMP Analysis

Amplitude-based and phase coherence analyses followed established practices for steady-state evoked potential analysis. Analyses were performed in

Matlab (R2020B). For each recording, Fast-Fourier Transforms (FFTs) were calculated for average waveforms, and amplitude values were obtained from the 37 Hz modulation frequency FFT bin. Signal-to-noise ratios (SNRs) were calculated with the amplitude of the modulation frequency FFT bin and the average amplitude of noise surrounding the modulation frequency (MF) ± 5 Hz. These same analyses were also conducted on harmonics of the MF. For objective response detection, SNR was used as an F-ratio with 2,10 degrees of freedom. A response was considered present if the SNR was greater than 6.13 dB ($p = 0.05$). Fig. 2 demonstrates this analysis approach using individual data. Offline, AMcVEMP amplitudes were corrected for the amount of mean, rectified EMG activity calculated over 0 to 1.024 ms

Phase coherence (PC) assesses the circular uniformity of phase angle of a given frequency (e.g., modulation frequency) from the individual, nonaveraged sweeps of each recording, using the Rayleigh test (Fisher 1993). It represents the degree of phase locking. PC is a similar measure to vector strength metrics used in single-unit studies of phase locking (Dobie & Wilson, 1989). FFTs were performed on each individual sweep. A perfectly identical phase angle for each sweep results in a phase coherence (PC) value of 1.0, whereas a value of 0 would indicate a random phase, and therefore an absent response. The PC criterion for response presence was 0.15 at an alpha level of 0.05 ($p=\exp(-nR^2)$) (Wianda & Ross, 2016). Figure 2 shows an example of an individual participant's polar histogram with corresponding phase coherence values; these values would constitute a present response.

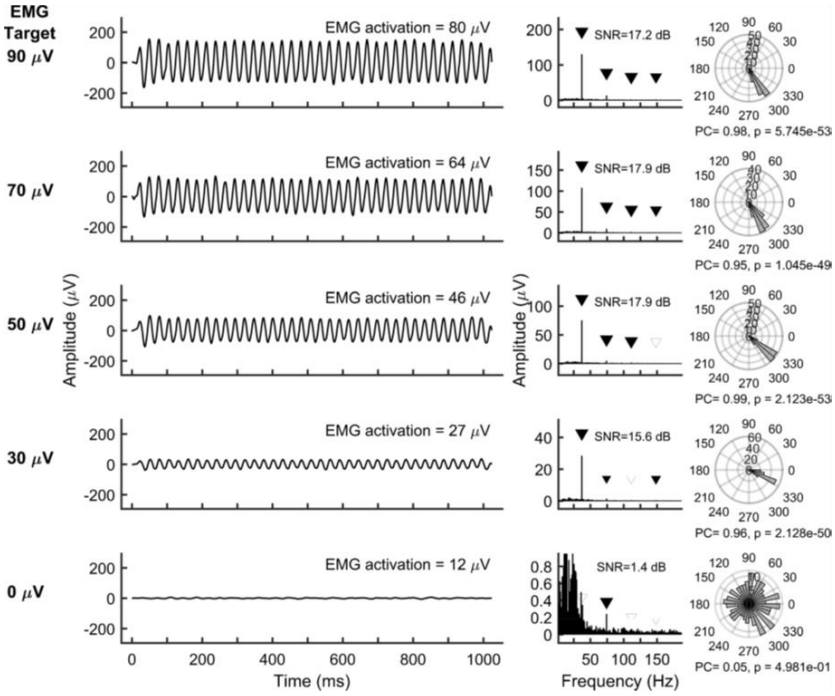

Figure 2*:* Individual AMcVEMP data from a young participant (21 years old) at five different EMG targets. ***Left Column,*** AMcVEMP response waveforms at 5 different EMG targets demonstrating 37 Hz periodicity. No response waveform is visible for the 10 μV EMG target. ***Middle Column,*** FFT of AMcVEMP response and harmonics at 5 different EMG targets; filled triangles represent present response, and open triangles represent absent responses. Response presence was confirmed by robust SNR (>6). Response presence was only noted for second harmonic at 10 μV EMG target. ***Right Column,*** Polar histograms of AMcVEMP response at 5 different EMG targets. Narrower histograms reflect better phase locking. PC = 1.0 represents perfect phase locking. No present response was noted for 10 μV condition.

Transient cVEMP Analysis

Peak-to-peak amplitudes and latencies of the p13 and n23 peaks were assessed in each participant using visual detection. Corrected amplitude values were calculated by comparing raw peak-to-peak amplitudes with the mean, rectified pre-stimulus EMG from -60 to 0 ms.

Statistical Approach

Statistical analyses were performed in SPSS (Version 27) and Matlab (R2020B). VEMP data were analyzed across EMG target (five levels) using repeated-measures analysis of variance (ANOVA). When comparing AM and transient cVEMPs, a 2 (VEMP type) x 5 (EMG targets) repeated measures ANOVA was used. Bonferroni corrections were used for post hoc p values. Greenhouse-Geiser corrections were used when appropriate. Partial-eta squared was used as a measure of effect size. Left and right sides were evaluated in separate ANOVAs.

Results

EMG Activation

All participants accurately reached tonic EMG target levels from 10 through 90 μV. Linear regression analysis revealed the significantly predictive relationship between EMG target and actual EMG activation (Fig. 3). EMG activation was symmetrical between left and right sides (Fig. 3.B,D).

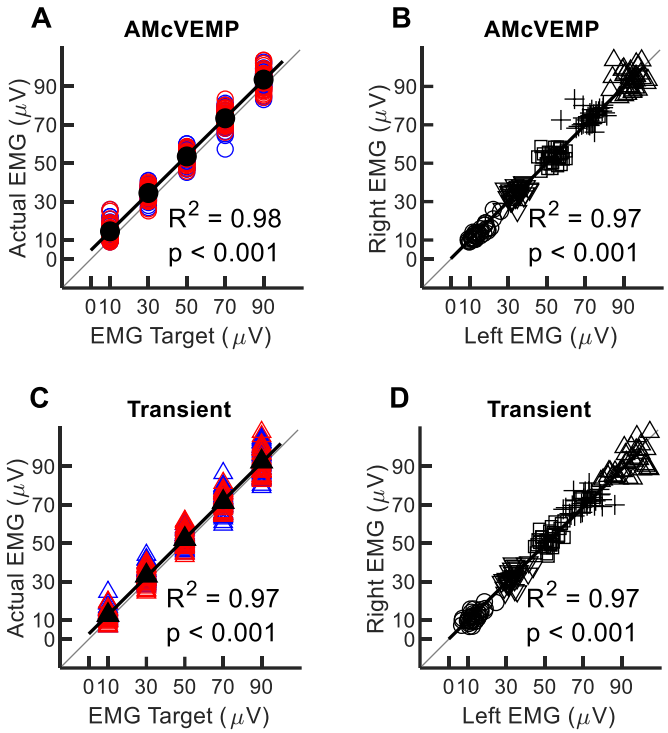

Figure 3*:* Scatterplots of EMG target and EMG activation. ***A***, AMcVEMP EMG activation as a function of EMG target for left (blue) and right (red) sides. Filled black symbols represent the combined average of both sides. The diagonal gray line represents the line of equality and the diagonal black line represents the best linear fit. ***B***, AMcVEMP EMG activation from the left and right sides (circles, 10 μV; downward triangles, 30 μV; squares, 50 μV; plus signs, 70 μV; upward triangles, 90 μV). ***C***, transient cVEMP EMG activation as a function of EMG target. ***D,*** Transient cVEMP EMG activation from left and right sides. Participants were able to accurately reach the EMG targets; EMG activation was more variable at the 90-μV EMG target. Activation from the left and right sides was symmetrical.

Amplitude

Raw Amplitude

Raw AMcVEMP amplitude increased linearly with EMG activation (Fig 4A-B), and this effect was significant [left: $F_{(1.25, 42.67)} = 133.685$, $p < .001$, partial $\eta^2 = .797$; right: $F_{(1.236, 42.034)} = 197.290$, $p < .001$, partial $\eta^2 = .853$]. Transient cVEMPs

were present in only six left ears and three right ears for the 10 µV EMG target; therefore repeated measures ANOVAs for transient cVEMP amplitude had only four levels (EMG targets of 30, 50, 70, and 90 µV). Raw transient cVEMP amplitude also significantly increased linearly with EMG activation (Fig 5A-B) and this effect was significant [left: $F_{(1.3, 41.6)} = 133.95$, $p < .001$, partial $\eta^2 = .807$; right: $F_{(1.35, 45.84)} = 123.49$, $p < .001$, partial $\eta^2 = .784$]. This behavior is consistent with transient cVEMP literature (Akin et al., 2004). Kernel density estimates for each type of cVEMP (Fig 4C, Fig 5C) showed very low amplitudes for the 10 µV EMG target, and broadly distributed amplitudes for higher EMG targets. Transient cVEMPs had larger amplitudes than AMcVEMPs (Fig 6A).

Corrected amplitudes

Corrected AMcVEMP amplitudes plateaued from 30-90 uV in both ears (Fig 4D-E). One-way repeated measures ANOVAs revealed a significant main effects of EMG target (5 levels) for left and right sides [left: $F_{(1.50, 50.90)} = 122.23$, $p < .001$, partial $\eta^2 = 782$; right: $F_{(1.47, 49.54)} = 171.49$, $p < .001$, partial $\eta^2 = .835$]. Corrected transient cVEMP amplitude also increased linearly with EMG activation (Fig 5A-B) and ANOVAs revealed a significant main effect of EMG target (four levels, 30 – 90 µV) [left: $F_{(2.15, 68.74)} = 22.33$, $p < .001$, partial $\eta^2 = .411$; right: $F_{(2.17, 73.65)} = 19.47$, $p < .001$, partial $\eta^2 = .364$]. Post-hoc comparisons within both ears revealed that corrected AMcVEMP amplitude at 10 and 30 µV were significantly different than each other and the higher EMG targets ($p < .001$), and that corrected AMcVEMP amplitudes from 50, 70, and 90 µV were not significantly different from each other (left: $p = .1.0$; right: $p = .802 – 1.0$). Kernel

density estimates for each type of cVEMP (Fig 4F, Fig 5F) showed very low corrected amplitudes for the 10 µV EMG target, and broadly distributed corrected amplitudes for higher EMG targets. Transient cVEMPs had larger amplitudes than AMcVEMPs (Fig. 6B).

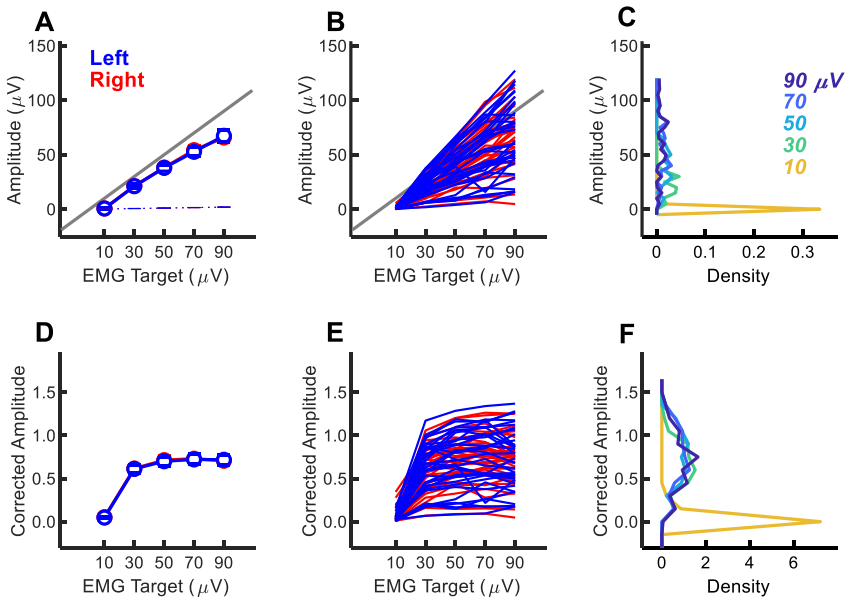

Figure 4*:* AMcVEMP amplitude across EMG targets. ***A***, average AMcVEMP amplitude (solid lines) and noise (dotted lines) for left (blue) and right (red) sides. The diagonal gray line represents the line of equality. ***B,*** Individual raw amplitude data for each side. ***C,*** Kernel density estimates of amplitude for each EMG target. ***D,*** average corrected AMcVEMP amplitude. ***E,*** individual corrected AMcVEMP amplitude. ***F,*** Kernel density estimates for corrected AMcVEMP amplitude.

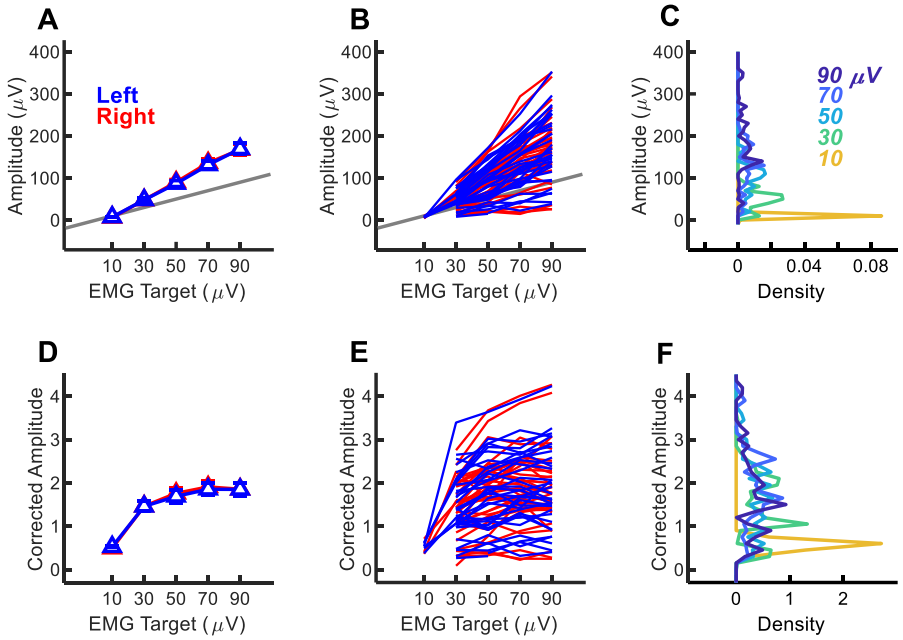

Figure 5: Transient cVEMP amplitude across EMG targets. ***A***, average AMcVEMP amplitude (solid lines) and noise (dotted lines) for left (blue) and right (red) sides. The diagonal gray line represents the line of equality. ***B***, Individual raw amplitude data for each side. ***C***, Kernel density estimates of amplitude for each EMG target. ***D***, average corrected transient cVEMP amplitude. ***E***, individual corrected transient cVEMP amplitude. ***F***, Kernel density estimates for corrected transient cVEMP amplitude.

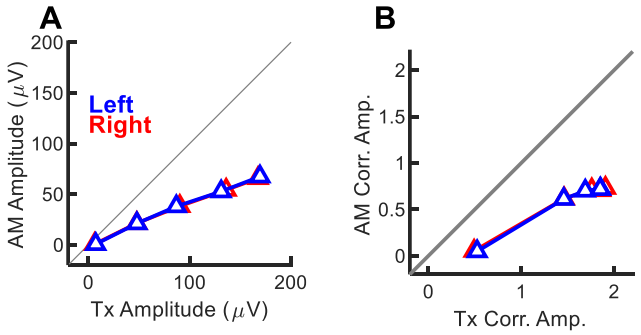

Figure 6*:* Scatterplots of AMcVEMP amplitude and transient cVEMP amplitude. ***A***, Average raw amplitude for left (blue) and right (red) sides. The diagonal gray line represents the line of equality. ***B,*** Average corrected amplitude for left (blue) and right (red) sides.

Signal to Noise Ratio

Cervical VEMP amplitudes, which represent an inhibition of tonic EMG activity (Colebatch & Rothwell, 2004), increase with higher EMG activation levels. Signal-averaged noise from the SCM muscle also increases with higher EMG activation. The result is a plateau in SNR from 30-90 µV, which was observed in the data set for this experiment (Fig. 7A-B) as well as for Clinard et al (2020).

One-way repeated measures ANOVAs revealed significant main effects of EMG target (5 levels) for left and right sides [left: $F_{(1.375, 46.738)} = 189.212$, $p < .001$, partial $\eta^2 = .848$; right: $F_{(1.217, 41.382)} = 143.646$, $p < .001$, partial $\eta^2 = .809$]. Post-hoc comparisons within both ears revealed that the SNR at 10 µV was significantly different than each higher EMG target ($p < .001$), and that SNRs from 30 to 90 µV were not significantly different from each other (left: $p = .950 – 1.00$; right: $p = .143 – 1.00$). One exception was found for the difference between the 30 and 50 µV EMG target, which was significant in the left ear ($p < .05$). SNR was not different between ears ($F_{(1.00, 35.00)} = .833$, $p = 0.368$). These findings were consistent for individual and group data (Fig. 7A-B). Kernel density estimates (Fig. 7C) showed broadly distributed SNRs for the 10 µV EMG target, and narrowly distributed SNRs for higher EMG targets.

Relationship Between Amplitude and Noise

Plotted on a log-linear axis, AMcVEMP amplitude and noise scaled in a linear fashion with EMG activation and remain parallel with one another from 30 to 90 µV (Fig. 8). Simple linear regression analyses performed on both

AMcVEMP amplitude and noise over the 30-, 50-, 70-, and 90- μV targets demonstrated significant predictive effects of EMG target on AMcVEMP. The slopes of the amplitude and noise regression formulae are similar, suggesting that amplitude and noise increased in a parallel fashion. Parallel growth in amplitude and noise would be expected to result in the SNR plateau from 30 to 90 μV which we observed for this experiment (Fig. 7)

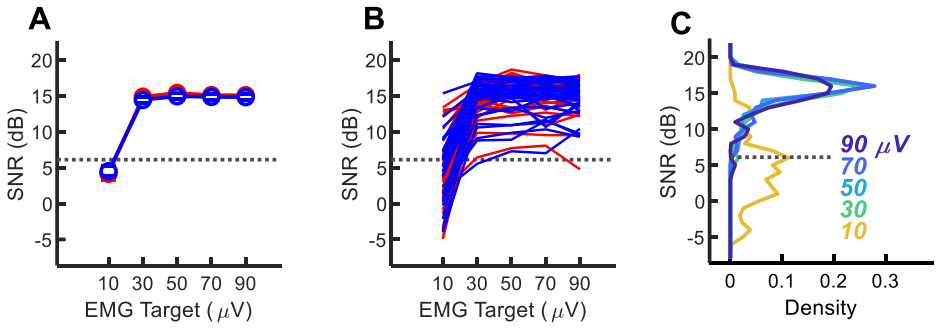

Figure 7: AMcVEMP SNR across EMG targets. ***A***, Average SNRs are shown for the Left and Right ears. The gray, dotted line indicates the SNR criterion for response presence. Errorbars represent one standard error. ***B***, Individual SNR data are shown from each ear. ***C***, Kernel density estimate plots.

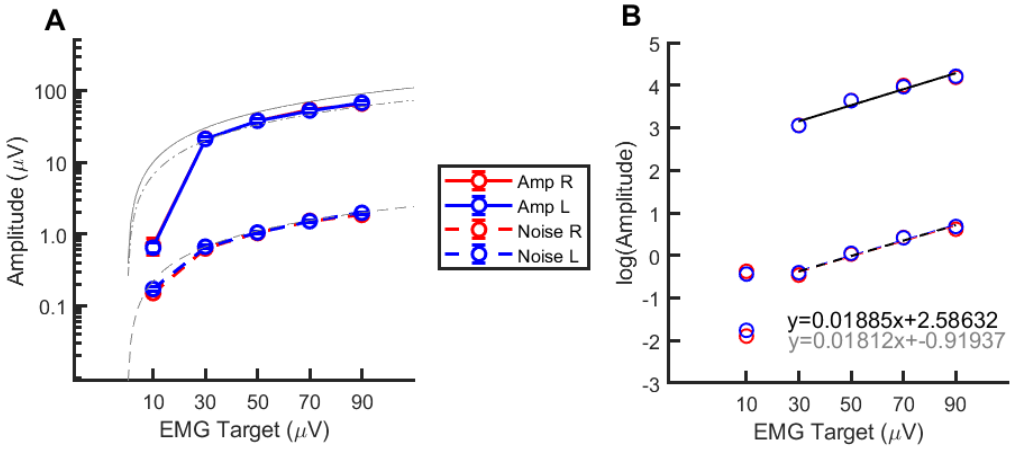

Figure 8: *A*, On a log-scaled y axis, amplitude and noise increase at parallel rates over EMG targets. The thin, gray line represents the line of equality; dashed gray lines represent linear changes. ***B***, Log-transformed amplitude and noise with linear regression from 30 to 90 µV EMG targets. The black line represents the linear fit to the left and right ear data. Regression slopes for amplitude (black) and noise (gray) are equivalent, consistent with the SNR plateau.

Phase Coherence

Prior to Clinard et al (2020), there were no published reports of phase-based synchrony measures from human cVEMPs. PC findings from this experiment replicated Clinard et al (2020).

PC was lowest for the 10 µV condition, but similarly to SNR, PC still exceeded the minimum cutoff criterion for a present response in some participants. PC nearly reached maximal levels (PC = 1.0) at 30 µV and remained approximately constant across 30, 50, 70, and 90 µV (Fig 9A-B). One-way repeated measures ANOVAs revealed significant main effects of EMG target (5 levels) within both sides [left: $F_{(1.340, 45.547)} = 203.285$, $p < .001$, $\eta^2 = .857$; right: $F_{(1.061, 36.066)} = 189.454$, $p < .001$, $\eta^2 = .848$]. PC was not significantly different across ears [$F_{(1.0, 35.00)} = .473$, $p = .496$]. Post-hoc analyses showed that PC at 10 µV was significantly different from every other EMG target ($p < .001$), but that the 30-90 µV conditions were not significantly different from each other ($p = .111 – 1.00$). One exception was found for the difference between the 50 and 90 µV EMG targets in the right ear, which was found to be significant ($p < .01$). Overall, PC plateaued in a similar manner to SNR from 30 to 90 µV. Kernel density estimates (Fig 9C) showed low PC values for the 10 µV EMG target, but narrowly distributed PC values approaching 1.0 for higher EMG targets.

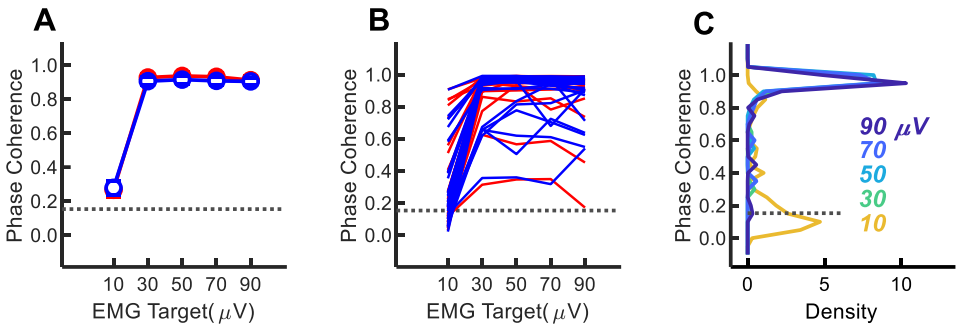

Figure 9*: A,* Phase coherence across EMG target. Average phase coherence is shown for **Left** and **Right** ears. Errorbars represent one standard error. The gray, dotted line indicates the criterion for response presence. ***B,*** Individual data are shown for each ear. ***C,*** Kernel density estimate plots.

Interaural Asymmetry Ratios

Results for IAR in this study closely replicate the findings of Clinard et al (2020). IARs were compared across EMG targets for each of the following AMcVEMP response analyses: raw amplitude, corrected amplitude, SNR, and PC. At the 10 μV target, IARs were similar across all analyses, although SNR and PC had some participants with larger asymmetries (Fig. 10_a). IARs ranges for each response analysis (i.e. SNR) were consistent across 30, 50, 70, and 90 μV targets (Fig. $10_{b\text{-}f}$). Raw and corrected amplitudes have similar IAR ranges, while SNR, PC, and phase angle showed comparatively much smaller and lower IAR ranges than either corrected or raw amplitude. Cutoff values for the upper range of normal, defined as two standard deviations greater than the mean (Papathanasiou et al., 2014) were calculated for each response analysis. Across all EMG targets greater than 10 μV, cutoff values were considerably lower for

SNR, PC, and phase angle than for raw or corrected amplitude. SNR and phase measurements could therefore be less susceptible to extraneous factors that may contribute to amplitude asymmetry (e.g. SCM size, SCM fatigue, electrode placement, transducer placement) (Sally M Rosengren et al., 2019), or could be inherently more symmetrical measures than amplitude even with all extraneous factors accounted for.

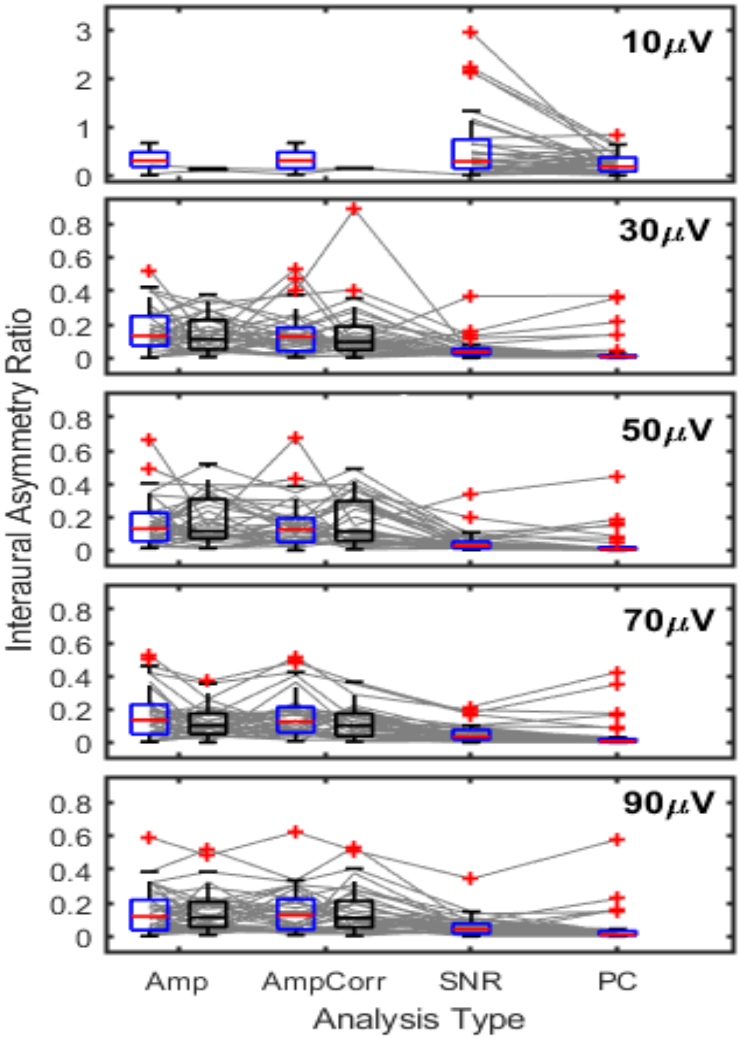

Figure 10: Boxplots of Asymmetry Ratios from each EMG target. The bottom and top of the box represent the 25th and 75th percentiles, respectively. The red horizontal line represents the median. Whiskers extend to the 1st and 99th percentiles. Outliers are represented by red plus symbols. Individual data are shown by thin, gray lines.

AMcVEMP Amplitude vs. Transient Amplitude

IARs were calculated for raw and corrected amplitudes for transient cVEMPs and were compared to IARs for AMcVEMPs. Amplitude-based IARs were similar across all EMG targets for both transient and AMcVEMPs (Fig. 10). AMcVEMP SNR and PC measures therefore demonstrated significantly lower IAR ranges than all amplitude measures calculated.

Discussion

Amplitude

Transient cVEMP and AMcVEMP Comparisons

AMcVEMP amplitudes from the present study and Clinard et al 2020 are larger than those recorded in previous literature (Bell et al., 2010; Oliveira et al., 2014). Corrected and uncorrected amplitudes were also lower overall for the present study compared to Clinard et al 2020 and did not approximate EMG target. The belly-SCM electrode junction montage used in this study results in a higher level of mean rectified EMG activation when compared to the bipolar electrode pair on the belly of the SCM used in Clinard et al 2020 (De Luca et al., 2012; Govender & Rosengren, 2021; Merletti et al., 2001). Participants were therefore able to reach EMG targets with less effort than in Clinard et al 2020, but the overall amount of underlying EMG was less by comparison. This resulted in lower overall cVEMP amplitudes.

Transient cVEMP amplitudes were larger than for AMcVEMPs (Fig. 6A-B), even though the tonebursts and AM tones were delivered at the same peak force

level, or dB pFL. Differences in stimulus rise time and envelope shape may have contributed to transient cVEMPs having larger amplitudes (Sally M. Rosengren et al., 2009). Longer rise times in stimulus envelopes have been shown to elicit less robust onset, transient cVEMPs (Sally M. Rosengren et al., 2009), and the rise time for a 37 Hz amplitude modulation is slower/longer than that of a 4-0-4 ms toneburst (Fig. 1). Clinical cVEMP stimulus and recording parameters and procedures lack standardization, making direct across-study comparisons of bone-conducted cVEMP amplitudes unfeasible (Mcnerney & Burkard, 2011).

SNR and Phase Coherence

SNR Plateaus

SNR reached maximal levels at 30 microvolts and plateaued through 90 uV, replicating the findings of Clinard et al (2020). This phenomenon was observed within individuals and in the overall average SNR (Fig. 7A-B). Average SNR values were also unchanged from Clinard et al (2020), remaining unaffected by the difference in electrode montage used. Parallel increases in AMcVEMP amplitude and signal-averaged noise, plotted on a log scale, are consistent with this plateauing effect seen in both studies. Spectral energy for cVEMP EMG is concentrated around 40 Hz (Lütkenhöner & Basel, 2012), which likely explains this proportional increase in noise vs. amplitude. Conventional cVEMP literature has also reported a similar plateauing effect for EMG-corrected amplitudes (Lütkenhöner et al., 2010; McCaslin et al., 2014; Sally M Rosengren, 2015; Tilburg et al., 2014) though this finding was only noted in the overall average amplitude (McCaslin et al., 2014).

Phase Coherence

High degrees of synchrony were observed in AMcVEMPs, regularly approaching a value of 1.0 (Fig. 9A-B). Like SNR, PC values also plateaued between 30 to 90 microvolts (mean value ~0.90), replicating Clinard et al (2020). Single-unit recordings of otolith afferent nerve fibers to 500 Hz stimuli demonstrated phase-locking abilities comparable to the PC values recorded from a far-field in this study (I. S. Curthoys et al., 2019; McCue & Jr, 1994). This high degree of synchrony in AMcVEMPs may be related to the function of the calyces of Type 1 vestibular hair cells (Songer & Eatock, 2013).

Clinical Implications

Advantages of Bone Conduction

Bone-conduction is an inherently more efficient otolith stimulus than air-conduction (Curthoys, 2010), and bone-conducted VEMPs have much lower thresholds in dB nHL than air-conducted cVEMPs (Mcnerney & Burkard, 2011; Welgampola et al., 2003). This results in BC VEMPs posing less risk of hearing damage due to noise exposure than AC VEMPs (Portnuff et al., 2017), an important consideration for VEMPs elicited by a constant, steady-state tone such as the one used in this study. An additional advantage of long-duration tones is the frequency specificity of the stimuli; the spectral energy of AM tones is more focused that transient toneburst spectra (Fig. 1) and may allow AMcVEMPs to provide a higher resolution methodology to assess cVEMP tuning properties, such as in aging and clinical populations

Maximum SNR and PC Reached With Low EMG

High levels of EMG activation were not necessary to reach maximal values for SNR and phase coherence (Fig. 7A-B, 9A-B). These measures plateaued from 30 to 90 µV, indicating that even modest levels of EMG activation result in maximal and consistent SNR and phase coherence. Evaluating SNR and PC measures with this method may allow for participants with physical comorbidities, such as limited cervical spine mobility, to be tested more easily. Cervical range of motion often becomes increasingly limited with age, which contributes to some elderly patients experiencing difficulty reaching even relatively low EMG levels of 50 µV (Akin et al., 2011). Clinically recommended EMG targets for transient cVEMPs often range from 50-200 µV (Papathanasiou et al., 2014; Sally M Rosengren, 2015). AMcVEMPs, and their minimal requirements for EMG activation, could provide a means to more easily test these aging populations. Although some responses were present at the 10 µV EMG target, the probability density functions for 10 µV show the majority of recordings had low SNRs consistent with absent responses.

Interaural Asymmetry Ratios are Lower for AMcVEMPs

Interaural Asymmetry Ratios are important for diagnostic cVEMP applications (Papathanasiou et al., 2014), especially in pathologies with unilateral presentations such as vestibular neuritis (Halmagyi et al., 2002), Meniere's disease (Taylor et al., 2011), superior semicircular canal dehiscence (Zuniga et al., 2013), and benign paroxysmal positional vertigo (Murofushi, 2016). Interaural asymmetry ratios for transient and AMcVEMP amplitudes were not

substantially different. However, IARs for SNR and PC were substantially smaller than both raw and corrected amplitudes for both AM and transient cVEMPs. The low IARs for SNR and PC measures may result in more sensitive clinical measures with better ROC curves compared to commonly used amplitude-based asymmetry calculations; AMcVEMPs have not yet been reported from clinical populations. Lower asymmetry ratios for SNR and PC may be related to their relative independence from EMG activation, at least over 30 to 90 µV.

Nonlinear Behavior of AMcVEMPs

Harmonic distortion products of the modulation frequency were present in AMcVEMPs of the present study. These distortion products may have their origin in the nonlinear processing of vestibular hair cells. Type 1 vestibular hair cells have rectifying behavior in animal saccules (Brown et al., 2017; Holt & Eatock, 1995; Sugihara & Furukawa, 1989) and auditory steady-state responses elicited by AM tones show similar harmonic distortion with origins consistent with rectification from inner hair cells (Picton et al., 2003). Auditory systems with impaired sensory cells are known to behave in a more linear fashion. Evaluating AMcVEMP distortion products could potentially yield useful information when diagnosing or assessing the progression of vestibular pathologies.

Amplitudes from the present study were lower than those of Clinard et al 2020; our previous work had amplitudes that approximated the EMG target. The present study used a different electrode montage, which affects the quantified level of EMG activation.

Conclusion

AMcVEMP and transient cVEMP amplitudes increased in linearly with higher EMG targets. For both VEMP types, corrected amplitude values remained relatively constant from 30 μV of EMG activation and above; AMcVEMP SNR and phase coherence values demonstrated similar plateaus from 30-90 μV of EMG activation. However, interaural asymmetry ratios for AMcVEMP SNR and phase coherence were significantly lower and less variable than either raw or corrected amplitude measures for transient cVEMPs and AMcVEMPs. Results of this study largely replicated the findings of Clinard et al (2020).

References

Akin, F. W., Murnane, O. D., Panus, P. C., Caruthers, S. K., Wilkinson, A. E., & Proffitt, T. M. (2004). The influence of voluntary tonic EMG level on the vestibular-evoked myogenic potential. *Journal of Rehabilitation Research and Development*, *41*, 473–480.

Akin, F. W., Murnane, O. D., Tampas, J. W., & Clinard, C. G. (2011). *The Effect of Age on the Vestibular Evoked Myogenic Potential and Sternocleidomastoid Muscle Tonic Electromyogram Level*. 617–622.

ANSI. (2004). *American National Standards Institute S3.6 - 2004 Specification for Audiometers*.

Bell, S. L., Fox, L., & Bihi, R. I. (2010). Vestibular evoked myogenic responses to amplitude modulated sounds. *The Journal of the Acoustical Society of America*, *128*(2), 559–562. https://doi.org/10.1121/1.3455831

Bogle, J. M., Zapala, D. A., Criter, R., & Burkard, R. (2013). The effect of muscle contraction level on the cervical vestibular evoked myogenic potential (cVEMP): Usefulness of amplitude normalization. *Journal of the American Academy of Audiology*, *24*(2), 77–88. https://doi.org/10.3766/jaaa.24.2.2

Brown, D. J., Pastras, C. J., & Curthoys, I. S. (2017). Electrophysiological measurements of peripheral vestibular function—A review of electrovestibulography. *Frontiers in Systems Neuroscience*, *11*(May), 1–17. https://doi.org/10.3389/fnsys.2017.00034

Clinard, C. G., Piker, E. G., Thorne, A. P., Surface, E. N., Anderson, A. E.,

Beacham, V. A., Crouse, M. C., Whitney, V. H., & Depaolis, R. A. (2019). Maximum Output and Low-Frequency Limitations of B71 and B81 Clinical Bone Vibrators: Implications for Vestibular Evoked Potentials. *Ear and Hearing*, *41*(4), 847–854. https://doi.org/10.1097/AUD.0000000000000808

Clinard, C. G., Thorne, A. P., & Piker, E. G. (2020). Effects of Tonic Muscle Activation on Amplitude-Modulated Cervical Vestibular Evoked Myogenic Potentials (AMcVEMPs) in Young Females: Preliminary Findings. *JARO - Journal of the Association for Research in Otolaryngology*, 1–17. https://doi.org/10.1007/s10162-020-00766-z

Colebatch, J. G., & Halmagyi, G. M. (1992). Vestibular evoked potentials in human neck muscles before and after unilateral vestibular deafferentation. *Neurology*, *42*(August), 1635–1636.

Colebatch, J. G., Halmagyi, G. M., & Skuse, N. F. (1994). Myogenic potentials generated by click-evoked vestibulocollic reflex. *Journal of Neurology, Neurosurgery, and Psychiatry*, *57*, 190–197.

Colebatch, J. G., & Rothwell, J. C. (2004). Motor unit excitability changes mediating vestibulocollic reflexes in the sternocleidomastoid muscle. *Clinical Neurophysiology*, *115*(11), 2567–2573. https://doi.org/10.1016/j.clinph.2004.06.012

Curthoys, I. S., Burgess, A. M., & Goonetilleke, S. C. (2019). Phase-locking of irregular guinea pig primary vestibular afferents to high frequency (>250 Hz) sound and vibration. *Hearing Research*, *373*, 59–70.

https://doi.org/10.1016/j.heares.2018.12.009

Curthoys, Ian S. (2010). Clinical Neurophysiology Invited review A critical review of the neurophysiological evidence underlying clinical vestibular testing using sound , vibration and galvanic stimuli. *Clinical Neurophysiology*, *121*(2), 132–144. https://doi.org/10.1016/j.clinph.2009.09.027

De Luca, C. J., Kuznetsov, M., Gilmore, L. D., & Roy, S. H. (2012). Inter-electrode spacing of surface EMG sensors: Reduction of crosstalk contamination during voluntary contractions. *Journal of Biomechanics*, *45*(3), 555–561. https://doi.org/10.1016/j.jbiomech.2011.11.010

Dobie, R. A., & Wilson, M. J. (1989). Analysis of auditory evoked potentials by magnitude-squared coherence. *Ear and Hearing*, *10*(1), 2–13. https://doi.org/10.1097/00003446-198902000-00002

Fisher, N. I. (1993). *Statistical analysis of Circular Data*. Cambridge University.

Govender, S., & Rosengren, S. M. (2021). Quantifying the effects of electrode placement and montage on measures of cVEMP amplitude and muscle contraction. *Journal of Vestibular Research: Equilibrium and Orientation*, *31*(1), 47–59. https://doi.org/10.3233/VES-200033

Halmagyi, G. M., Aw, S. T., Karlberg M, Curthoys, I. S., & Todd, M. J. (2002). Inferior vestibular neuritis. *New York Academy of Sciences*, *956*, 306–313. https://doi.org/10.1007/s00415-011-6375-4

Holt, J. R., & Eatock, R. A. (1995). Inwardly rectifying currents of saccular hair

cells from the leopard frog. *Journal of Neurophysiology*, *73*(4), 1484–1502. https://doi.org/10.1152/jn.1995.73.4.1484

Jaramillo, F., Markin, V. S., & Hudspeth, A. J. (1993). Auditory illusions and the single hair cell. *Nature*, *364*(6437), 527–529. https://doi.org/10.1038/364527a0

Kozlov, A. S., Baumgart, J., Risler, T., Versteegh, C. P. C., & Hudspeth, A. J. (2011). Forces between clustered stereocilia minimize friction in the ear on a subnanometre scale. *Nature*, *474*(7351), 376–379. https://doi.org/10.1038/nature10073

Kozlov, A. S., Risler, T., Hinterwirth, A. J., & Hudspeth, A. J. (2012). Relative stereociliary motion in a hair bundle opposes amplification at distortion frequencies. *Journal of Physiology*, *590*(2), 301–308. https://doi.org/10.1113/jphysiol.2011.218362

Li, C., Layman, A. J., Carey, J. P., & Agrawal, Y. (2015). Epidemiology of vestibular evoked myogenic potentials: Data from the Baltimore Longitudinal Study of Aging. *Clinical Neurophysiology*, *126*(11), 2207–2215. https://doi.org/10.1016/j.clinph.2015.01.008

Lim, C. L., Clouston, P., Sheean, G., & Yiannikas, C. (1995). The Influence of Voluntary EMG Activty and Click Intensity On the Vestibular Click Evoked Myogenic Potential. *Muscle and Nerve*, *18*, 1210–1213.

Lütkenhöner, B., & Basel, T. (2012). Deconvolution of the vestibular evoked myogenic potential. *Journal of Theoretical Biology*, *294*, 87–97.

https://doi.org/10.1016/j.jtbi.2011.10.033

Lütkenhöner, B., Stoll, W., & Basel, T. (2010). Modeling the vestibular evoked myogenic potential. *Journal of Theoretical Biology*, *263*(1), 70–78. https://doi.org/10.1016/j.jtbi.2009.10.036

McCaslin, D. L., Fowler, A., & Jacobson, G. P. (2014). Amplitude normalization reduces Cervical Vestibular Evoked Myogenic Potential (cVEMP) amplitude asymmetries in normal subjects: Proof of concept. *Journal of the American Academy of Audiology*, *25*(3), 268–277. https://doi.org/10.3766/jaaa.25.3.6

McCue, M. P., & Jr, J. J. G. (1994). *Acoustically Responsive Fibers in the Vestibular Nerve of the Cat*. *14*(October), 6058–6070.

Mcnerney, K. M., & Burkard, R. F. (2011). *The Vestibular Evoked Myogenic Potential (VEMP): Air- Versus Bone-Conducted Stimuli*. 6–15.

Merletti, R., Rainoldi, A., & Farina, D. (2001). Surface electromyography for noninvasive characterization of muscle. *Exercise and Sport Sciences Reviews*, *29*(1), 20–25. https://doi.org/10.1097/00003677-200101000-00005

Murofushi, T. (2016). Clinical application of vestibular evoked myogenic potential (VEMP). *Auris Nasus Larynx*, *43*(4), 367–376. https://doi.org/10.1016/j.anl.2015.12.006

Noij, K. S., Herrmann, S., & Rauch, D. (2017). Toward Optimizing Vestibular Evoked Myogenic Potentials : Normalization Reduces the Need for Strong Neck Muscle Contraction. *Audiology & Neurotology*, *22*, 282–291.

https://doi.org/10.1159/000485022

Oliveira, A. C. De, Pereira, L. D., Fernando, J., & Menezes, P. D. L. (2014). Amplitude modulated vestibular evoked myogenic responses : a study of carrier and modulating frequencies. *Acta Oto-Laryngologica*, *134*, 796–801. https://doi.org/10.3109/00016489.2014.909605

Papathanasiou, E. S., Murofushi, T., Akin, F. W., & Colebatch, J. G. (2014). International guidelines for the clinical application of cervical vestibular evoked myogenic potentials: an expert consensus report. *Clin Neurophysiol*, *125*(4), 658–666. https://doi.org/10.1016/j.clinph.2013.11.042

Pastras, C. J., Curthoys, I. S., & Brown, D. J. (2017). In vivo recording of the vestibular microphonic in mammals. *Hearing Research*, *354*, 38–47. https://doi.org/10.1016/j.heares.2017.07.015

Picton, T. W., John, M. S., Dimitrijevic, A., & Purcell, D. (2003). Human auditory steady-state responses. *International Journal of Audiology*, *42*(4), 177–219. https://doi.org/10.3109/14992020309101316

Portnuff, C. D. F., Kleindienst, S., & Bogle, J. M. (2017). Safe use of acoustic vestibular-evoked myogenic potential stimuli: Protocol and patient-specific considerations. *Journal of the American Academy of Audiology*, *28*(8), 708–717. https://doi.org/10.3766/jaaa.16071

Romero, D. J., Piker, E. G., Thorne, A., & Clinard, C. (2021). Comparison of Bone-Conducted Cervical VEMPs Elicited by B71 and B81 Bone Vibrators. *Ear and Hearing*, *42*(3), 596–605.

https://doi.org/10.1097/AUD.0000000000000978

Rosengren, S M, Welgampola, M. S., & Colebatch, J. G. (2010). Clinical Neurophysiology Vestibular evoked myogenic potentials : Past , present and future. *Clinical Neurophysiology*, *121*(5), 636–651. https://doi.org/10.1016/j.clinph.2009.10.016

Rosengren, Sally M., Govender, S., & Colebatch, J. G. (2009). The relative effectiveness of different stimulus waveforms in evoking VEMPs: Significance of stimulus energy and frequency. *Journal of Vestibular Research: Equilibrium and Orientation*, *19*(1–2), 33–40. https://doi.org/10.3233/VES-2009-0345

Rosengren, Sally M. (2015). Clinical Neurophysiology Effects of muscle contraction on cervical vestibular evoked myogenic potentials in normal subjects. *Clinical Neurophysiology*, *126*(11), 2198–2206. https://doi.org/10.1016/j.clinph.2014.12.027

Rosengren, Sally M, Colebatch, J. G., Young, A. S., Govender, S., & Welgampola, M. S. (2019). Clinical Neurophysiology Practice Vestibular evoked myogenic potentials in practice : Methods , pitfalls and clinical applications. *Clinical Neurophysiology Practice*, *4*, 47–68. https://doi.org/10.1016/j.cnp.2019.01.005

Songer, J. E., & Eatock, R. A. (2013). Tuning and timing in mammalian type i hair cells and calyceal synapses. *Journal of Neuroscience*, *33*(8), 3706–3724. https://doi.org/10.1523/JNEUROSCI.4067-12.2013

Sugihara, I., & Furukawa, T. (1989). Morphological and functional aspects of two different types of hair cells in the goldfish sacculus. *Journal of Neurophysiology*, *62*(6), 1330–1343. https://doi.org/10.1152/jn.1989.62.6.1330

Taylor, R. L., Wijewardene, A. A., Gibson, W. P. R., Black, D. A., Halmagyi, G. M., & Welgampola, M. S. (2011). The vestibular evoked-potential profile of Ménière's disease. *Clinical Neurophysiology*, *122*(6), 1256–1263. https://doi.org/10.1016/j.clinph.2010.11.009

Tilburg, M. J. Van, Herrmann, B. S., Jr, J. J. G., & Rauch, S. D. (2014). *Normalization Reduces Intersubject Variability in Cervical Vestibular Evoked Myogenic Potentials*. 222–227.

Welgampola, M. S., Rosengren, S. M., Halmagyi, G. M., & Colebatch, J. G. (2003). *Vestibular activation by bone conducted sound*. J Neurol Neurosurg Psychiatry 2003;74:771–778

Wianda, E., & Ross, B. (2016). Detecting neuromagnetic synchrony in the presence of noise. *Journal of Neuroscience Methods*, *262*, 41–55. https://doi.org/10.1016/j.jneumeth.2016.01.012

Zuniga, M. G., Janky, K. L., Nguyen, K. D., Welgampola, M. S., & Carey, J. P. (2013). Ocular versus cervical VEMPs in the diagnosis of superior semicircular canal dehiscence syndrome. *Otology and Neurotology*, *34*(1), 121–126. https://doi.org/10.1097/MAO.0b013e31827136b0